LBL-28022
Preprint

# Lawrence Berkeley Laboratory
UNIVERSITY OF CALIFORNIA

## APPLIED SCIENCE DIVISION

Submitted to Atmospheric Environment

# Transport and Deposition of Indoor Radon Decay Products: Part 1 — Model Development and Validation

G.E. Schiller, A.V. Nero, and C.L. Tien

August 1989

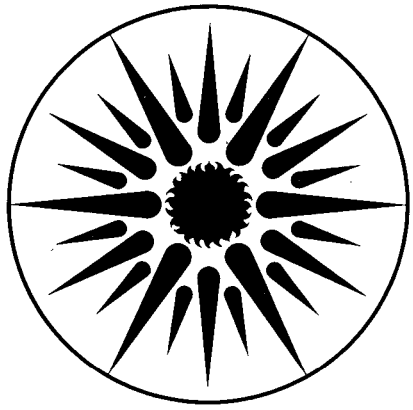

**APPLIED SCIENCE DIVISION**



**Prepared for the U.S. Department of Energy under Contract Number DE-AC03-76SF00098.**

## DISCLAIMER

LBL-28022

Submitted to:
*Atmospheric Environment*

# Transport and Deposition of Indoor Radon Decay Products: Part 1 -- Model Development and Validation

G.E. Schiller[1], A.V. Nero[2], and C.L. Tien[3]

[1]Building Science Group
Department of Architecture
University of California at Berkeley
Berkeley, CA 94720

[2]Indoor Environment Program
Applied Science Division
Lawrence Berkeley Laboratory
1 Cyclotron Road
Berkeley, CA 94720

[3]Mechanical Engineering Department
University of California at Irvine
Irvine, CA 92717

August 1989

This work was supported by the Director, Office of Energy Research, Office of Health and Environmental Research, Pollutant Characterization and Safety Research Division, and by the Assistant Secretary for Conservation and Renewable Energy, Office of Buildings and Community Systems, Building Systems Division, of the U.S. Department of Energy under Contract No. DE-AC03-76SF00098.

# TRANSPORT AND DEPOSITION OF INDOOR RADON DECAY PRODUCTS: Part 1 - Model Development and Validation

G.E. Schiller[1], A.V. Nero[2], C.L. Tien[3]

## ABSTRACT

Commonly used mathematical models of indoor radon decay product behavior are based on macroscopic mass-balances, often referred to as "uniformly-mixed models". The uniformly-mixed model's applicability is limited by its inability to track the movement of pollutants from their sources to other areas within the enclosure, to permit spatial- or time-dependent sources, or to take proper account of interactions with macroscopic surfaces. Although the uniformly-mixed model parameterizes the deposition process as a constant volumetric removal rate, in reality the deposition process is actually a surface phenomenon and is strongly affected by environmental conditions.

This paper describes the development of RADTRAN, a two-dimensional radon progeny transport model that begins with the differential conservation equations describing the motion of air and the transport of reactive pollutants, introduces appropriate boundary conditions to represent surface deposition, and then calculates the concentration distribution of radon progeny throughout the entire region of interest. Knowing the concentration gradient near the surface, a local mass-transfer coefficient (the deposition velocity) can be determined as a function of environmental conditions. RADTRAN simulations have been based on several flow conditions: buoyancy-driven recirculating enclosure flows, free and forced-convection boundary layer flows, and one-dimensional diffusion. Free progeny diffusivity, $D^f$, and attachment rate, $X$, were varied over representative ranges. For these conditions, RADTRAN calculated free deposition velocities of $u^f$ = 0.014 - 0.079 cm/sec, for $^{218}Po$. RADTRAN predictions are compared to a range of experimental measurements. It was found that the predicted range of deposition velocities is in rough agreement with findings from experiments conducted in flow conditions similar to the simplified flows used in RADTRAN.

Keywords: radon progeny, indoor environment, deposition, diffusion, convection, modeling, prediction

[1] Dr. Schiller is an Assistant Professor in the Building Science Group of the Dept. of Architecture, University of California, Berkeley, and a Faculty Associate in the Applied Science Division, Lawrence Berkeley Laboratory, California.
[2] Dr. Nero is a Staff Scientist in the Radon Group of the Indoor Environment Program, Applied Science Division, Lawrence Berkeley Laboratory, California.
[3] Dr. Tien is a Professor of Mechanical Engineering, and Executive Vice-Chancellor of the University of California, Irvine.

# TRANSPORT AND DEPOSITION OF INDOOR RADON DECAY PRODUCTS: Part 1 - Model Development and Validation

G.E. Schiller[1], A.V. Nero[2], C.L. Tien[3]

## 1.0 INTRODUCTION

Radon-222 ($^{222}Rn$), a naturally occurring radioactive gas, is currently recognized as a significant public health hazard. Nazaroff and Teichman (1989) estimate that 16,000 lung-cancer deaths per year in the U.S. can be attributed to radon decay product exposure. The radon decay chain is shown in Figure 1. The first four decay products - $^{218}Po$, $^{214}Pb$, $^{214}Bi$, and $^{214}Po$ - are chemically active and pose a significant health risk due to their short half-lives. When inhaled, they can deposit in the lung and subsequently irradiate the surrounding tissue before being removed by lung clearance mechanisms. Because $^{214}Po$ has such a short half-life, for practical purposes it is considered to always be in equilibrium with $^{214}Bi$. For biological considerations, the decay chain effectively ends with the 5th decay product, $^{210}Pb$, because of its long half-life of 22 years.

Being an inert gas, $^{222}Rn$ is treated as essentially stable due to its relatively long half-life, and its concentration is typically uniform within a single room unless the ventilation rate is quite high. In contrast, the behavior of radon decay products indoors is extremely complex, involving interactions with trace gases, airborne particles and room surfaces. The first decay product, $^{218}Po$, initially exists as a single free ion but develops rapidly into a small molecular cluster commonly referred to as the "free" activity mode (Phillips et al., 1988). These decay products may become attached to pre-existing airborne particles, whose size distribution therefore determines that of the "attached" decay products in the space. Recent investigations suggest that a third "nucleation" mode exists, caused by clustering of binary mixtures of condensable products (e.g., $H_2SO_4$ and $H_2O$). This increased growth is called ion-induced aerosol formation and serves to broaden the size distribution of the free fraction (Raes et al., 1985, 1987). The work presented in this paper uses the bimodal description of the activity size distribution, while recognizing that this middle nucleation mode might account for some of the observed range of diffusion coefficients associated with the free progeny.

Distinguishing between the behavior of the free and attached progeny is important for two reasons. First, the size distribution has biological implications by affecting both the extent to which the radioactive decay products pass through various parts of the human respiratory system, and the likelihood of deposition onto sensitive tissues. Second, the size distribution influences, and is also partially determined by, the rate of transport and deposition of the pollutants within the room. The deposition of radon progeny onto walls and other surfaces is an important removal mechanism at the low to moderate particle concentrations typically found indoors (Jacobi, 1972; Pörstendorfer et al., 1978a; Sextro et al., 1986). This rate of removal can be large for free progeny, but is

[1] Dr. Schiller is an Assistant Professor in the Building Science Group of the Dept. of Architecture, University of California, Berkeley, and a Faculty Associate in the Applied Science Division, Lawrence Berkeley Laboratory, California.
[2] Dr. Nero is a Staff Scientist in the Radon Group of the Indoor Environment Program, Applied Science Division, Lawrence Berkeley Laboratory, California.
[3] Dr. Tien is a Professor of Mechanical Engineering, and Executive Vice-Chancellor of the University of California, Irvine.

approximately two orders of magnitude smaller for the attached progeny due to their larger size and correspondingly smaller diffusivity. Deposition is often described in terms of the deposition velocity, defined later in this paper. For a more detailed discussion of the behavior of indoor radon and its decay products, Nazaroff & Nero (1988) provide a substantive review of our current understanding of the indoor radon problem.

Interest in the behavior, health implications, and potential control strategies of indoor radon progeny has generated a broad range of research investigations taking many different approaches. These include epidemiological studies, geologic surveys, monitoring in homes, full-scale experiments, and mathematical modeling. The most commonly used mathematical models of indoor radon decay product behavior are based on macroscopic mass-balances, often referred to as "uniformly-mixed models" or "box models" (Jacobi, 1972; Pörstendorfer et al., 1978a; Wicke et al., 1981; Bruno 1983; Knutson et al., 1983). In their steady-state form, these models give rise to simple algebraic equations that have no spatial or temporal dependence and are easily solved. The uniformly-mixed model is typically used for analyzing experimental data, estimating overall conditions in rooms, or running simple parametric studies. However, it is only able to characterize the average concentrations in a room, and does not consider the actual mechanisms of the transport and removal processes. As a result, the model's applicability is limited by its inability to track the movement of pollutants from their sources to other areas within the enclosure, to permit spatial- or time-dependent sources, or to take proper account of interactions with macroscopic surfaces. Although the uniformly-mixed model parameterizes the deposition process as a constant volumetric removal rate, in reality the deposition process is actually a surface phenomenon and is strongly affected by environmental conditions. As a result, there is wide variability found among researchers' experimentally determined values of deposition rates.

This paper describes the development of RADTRAN, a two-dimensional radon progeny transport model that begins with the differential conservation equations describing the motion of air and the transport of reactive pollutants, introduces appropriate boundary conditions to represent surface deposition, and then calculates the concentration distribution throughout the entire region of interest. Fundamental mass-transport equations separately describe the free and attached concentrations of each of the first three radon decay products in terms of their generation, convective and diffusive transport, and removal. The equations are coupled through source and removal terms. The two-dimensional velocity fields in the space are assumed to be independent of the pollutant concentrations, and are obtained separately and used as input to the mass-transport equations. Air flow regimes analyzed include free and forced boundary layer flows and two-dimensional buoyancy-driven enclosure flows, for laminar conditions. The solution of the mathematical formulation of the model is based on an approximating numerical technique. Knowing the concentration gradient near the surface, a local mass-transfer coefficient (the deposition velocity) and the overall deposition rate for the space can be determined as a function of environmental conditions. As compared to the uniformly-mixed model, RADTRAN treats the deposition process in a more fundamental manner. By treating transport and removal directly, rather than by lumped parameterization, the approach used in RADTRAN is an important step in providing a realistic basis for understanding radon progeny behavior and its dependence on physical and environmental conditions.

## 2.0 FORMULATION OF THE MASS-TRANSPORT MODEL

The generalized mass-transport equation for any component, i, of a mixture is a differential equation derived by applying the law of conservation of mass to component i in an infinitesimal volume fixed in space. A transport law (Fick's first law of diffusion) is introduced so that the equation is written in terms of a single dependent variable (i.e., concentration). The component can be carried through this volume element by convective transport and also by diffusion. Both modes of transport depend on factors that are functions of time and space. Within the volume element, component i may also be created and destroyed by transformation processes represented as source and removal terms in the differential equation.

### *2.1 Mass-Transport Equations*

For radon decay products, transformations taking place throughout the entire region of interest include radioactive decay, attachment, and recoil. For notational convenience, superscripts f and a are used to designate the free and attached decay products, and subscripts 0, 1, 2, and 3 are used to represent $^{222}Rn$ and its first three decay products. Using vector notation, and writing in terms of activity concentration, $A=\lambda C$, the two-dimensional transport equations for decay product i (i=1,2,3) are presented below in equations (1a) and (1b).

$$\partial A_i^f/\partial t + u\cdot\nabla A_i^f - \nabla\cdot(D^f\nabla A_i^f) = [\,\lambda_i A_{i-1}^f + r_{i-1}\lambda_i A_{i-1}^a\,] - (\lambda_i + X) A_i^f \quad (1a)$$

$$\partial A_i^a/\partial t + u\cdot\nabla A_i^a - \nabla\cdot(D^a\nabla A_i^a) = [\,(1-r_{i-1})\lambda_i A_{i-1}^a + X A_i^f\,] - \lambda_i A_i^a \quad (1b)$$

where u is the air velocity, D is the coefficient of Brownian diffusivity, $\lambda$ is the radioactive decay constant, r is the recoil probability, and X is the attachment rate constant. The terms on the left side of these equations represent, respectively, the time rate of change of activity concentration of component i, convective transport, and diffusive transport. If the diffusion coefficients of the free and attached progeny are constant over space, then the third term on the left can be written as $D\nabla^2 A$.

The right side of each equation represents the net production of the free and attached progeny, represented by the source terms (parent atom decay, recoil for the free mode, attachment for the attached mode) minus the removal terms (decay, attachment for the free mode, recoil for the attached mode). The model first solves equation (1a), then (1b), for each decay product. The bracketed term on the right side of each equation is therefore a known quantity, and the equations can be solved for the concentration distributions of $A_i^f$ and $A_i^a$.

Values of the radioactive decay rate constants, $\lambda$, are obtained by the relation $\lambda = \ln 2/t_{1/2}$, where $t_{1/2}$ are the half-lives given in Figure 1. The attachment of radon progeny to particles is commonly described by the overall attachment rate X, a function of airvorne particle concentration N and size distribution (Pörstendorfer et al., 1978b). As in the uniformly-mixed model, the value of X in RADTRAN is obtained by assuming a linear relationship between X and N, with a constant coefficient of proportionality (the attachment coefficient) based on mean particle diameter. During preliminary simulations, X(x,y) was represented as a function of the spatial coordinates x and y, by first solving for the spatial distribution of particle concentration N(x,y). The variation of X within the particle boundary layer did not affect the calculated value of deposition velocity, however, and so X was assumed to be constant in the subsequent simulations for which results are reported here. RADTRAN does

not contribute anything new to understanding the actual attachment process but only its implications in terms of concentration distributions and deposition rates. RADTRAN also treats the recoil process in the same way as previous models (Mercer, 1976), and presently assumes a constant recoil probability of $r_1 = 0.83$ for alpha decay, and $r_2 = r_3 = 0$ for beta decay.

The solution of these equations requires specification of initial conditions and boundary conditions. Since radon (i=0) is an inert gas, initial conditions of these recursion expressions are $A_o^f = A_o$, and $A_o^a = 0$. The radon concentration, $A_o$, serves as the initial source distribution for all the progeny, and can be any function of time or space. Boundary conditions represent surface reactions occurring at a specified edge of the region being considered. In general, boundary conditions can be expressed in terms of a specified concentration or flux at a surface, or as a mass flux written in terms of a mass-transfer coefficient or surface reaction rate (Bird et al., 1960). Since the walls are not considered as a source of radon in this model, the boundary conditions represent the deposition of radon decay products onto the surfaces of the space. This treatment is described in detail in section 3.0.

*2.2 Dimensionless Equations*

For convenience, the governing equations can be expressed in terms of dimensionless variables. These dimensionless variables are defined by dividing the variables in equations (1a) and (1b) by constant reference parameters chosen to be characteristic of the particular problem (i.e., radon concentration $A_o$, surface length L, representative velocity U, time step $\Delta t_o$). The governing equations, together with the initial and boundary conditions, are then formulated in terms of these non-dimensional variables. After rearranging, the resulting form of the equations contain important dimensionless combinations of the characteristic parameters. The non-dimensional form of the governing equations can be written as:

$$R\,\partial\theta_i^f/\partial\tau + f\bullet\nabla\theta_i^f - (1/ReSc)\,\nabla^2\theta_i^f = R\,(S1_i^f - S2_i^f\,\theta_i^f) \qquad (2a)$$

$$R\,\partial\theta_i^a/\partial\tau + f\bullet\nabla\theta_i^a - (1/ReSc)\,\nabla^2\theta_i^a = R\,(S1_i^a - S2_i^a\,\theta_i^a) \qquad (2b)$$

where it has been assumed that the diffusion coefficients are constant. In these equations, the gradient operators are in terms of dimensionless spatial coordinates based on the characteristic surface length, L, and the dimensionless parameters are defined below:

| dimensionless quantity | equivalent parameters | physical significance |
|---|---|---|
| $\theta$ | $A/A_o$ | activity concentration |
| f | $u/U$ | velocity vector |
| $\tau$ | $t/\Delta t_o$ | time |
| $R$ | $L/U\Delta t_o$ | N/A |
| Re | $LU/\nu$ | Reynolds number |
| Sc | $\nu/D$ | Schmidt number |
| $S1_i^f$ | $[\lambda_i\,\theta_{i-1}^f + r_{i-1}\,\lambda_i\,\theta_{i-1}^a]\cdot(\Delta t_o)$ | free source term |
| $S2_i^f$ | $(\lambda_i + X)\cdot(\Delta t_o)$ | free sink term |
| $S1_i^a$ | $[(1-r_{i-1})\,\lambda_i\,\theta_{i-1}^a + X\,\theta_i^f]\cdot(\Delta t_o)$ | attached source term |
| $S2_i^a$ | $(\lambda_i)\cdot(\Delta t_o)$ | attached sink term |

### *2.3 Numerical Solution Technique*

The coupled mass-transport equations in RADTRAN are non-linear, partial differential equations and cannot be solved analytically. The approximating numerical technique chosen here, the Patankar-Spalding differencing technique (Patankar, 1980), involves the conversion of each equation into discrete form (discretization) and a matrix solution of the resulting algebraic equations. The region of interest is divided into a finite number of contiguous subregions (control volumes), each represented by a unique grid point. To minimize computing costs a non-uniform grid is used with a fine grid spacing in the regions near the wall, where the largest spatial variations in concentrations occur, with a coarser grid in the core region of the room. There are 31 grid points along a length of the two-dimensional enclosure, with the dimensionless grid spacing ranging from 0.0022 near the wall to 0.132 in the center. The time period of interest is also divided into a finite number of one-minute timesteps.

The discretization method replaces a continuous distribution of the dependent variable (activity concentration, A) with discrete values at each grid point and for each time step. The values for A at the grid points are connected through the discretization equation, derived by integrating equations (2a) and (2b) over the control volume surrounding the grid point, and over the time step. In RADTRAN, the discretization equations are based on a hybrid scheme for the spatial profiles, accounting for the direction and relative magnitude of convection at each node (Patankar, 1980), and an implicit scheme for the transient profile. The discretization equations used in RADTRAN are summarized in Schiller (1984), written in terms of the dimensionless parameters used in equations (2a) and (2b).

For a region represented by M nodes, the differential equation is replaced by a set of M algebraic equations forming a matrix of coefficients that can be solved by any suitable method. Because each node is linked only to its neighboring nodes, the resulting matrix is very sparse and one can use relatively simple and fast iterative methods of solution. RADTRAN uses a line-by-line iterative solution technique, the alternating-direction implicit method, generating sets of tri-diagonal matrices (Patankar, 1980). The algorithms for inverting a tri-diagonal matrix are a simplified form of the standard Gaussian-elimination method, and are commonly referred to as the Tri-Diagonal Matrix Algorithm. An iterative solution marches through the time steps to produce the time-dependent concentration distribution. The iterations are repeated until steady-state is reached (determined in this case when the differences in concentrations between iterations is less than 0.1% for each grid point).

## 3.0 DEPOSITION

RADTRAN accounts for deposition through boundary conditions at the wall, instead of the overall deposition rate constant used in the uniformly-mixed model. When a particle (or an unattached decay product) collides with a surface it sticks, or deposits, on that surface. The interaction between the particle and the wall, and the probability of particle attachment, is often described in terms of an accommodation coefficient. Perfect

adherence at the wall is represented by an accommodation coefficient equal to one. There is also a probability of radiation-induced recoil from the wall. Bruno (1983) demonstrates that the recoil distance for alpha decay is approximately .015 cm, much less than the typical boundary layer thickness near the wall, and concludes that a recoiling nucleus that detaches from the wall is likely to be redeposited. RADTRAN assumes the wall to be a perfect sink, so that particles adhere perfectly to the surface without returning to a state of suspension.

Assuming that particles touching the wall are removed from the air implies that the airborne pollutant activity concentration at the surface ($A_s$) can be taken as zero (Fuchs, 1964), and that there exists a thin wall region over which the concentration increases to the freestream, or core, value ($A_c$). The thickness of the wall region depends on the relative magnitudes of the source and removal terms within the space (radioactive decay and attachment), the diffusion coefficient, and also the intensity of convection contributing to the transport of pollutants either towards or away from the wall. The resulting concentration gradient in this wall layer causes a continuous diffusion of pollutants towards the surface (Hinds, 1982). Deposition of particles can be due to the influence of many processes other than molecular diffusion, including turbulent (eddy) diffusion, gravitational settling, inertial impaction, electrostatic attraction (electrophoresis), and thermophoresis. The present formulation of RADTRAN accounts for deposition only by molecular diffusion, as discussed below. A brief discussion of the potential significance of the other deposition mechanisms follows in section 3.2.

### *3.1 Molecular Diffusion*

Molecular diffusion is the net transport of particles in a concentration gradient due to random Brownian motion. Diffusion increases in magnitude for smaller particle diameter and, excluding convection, is the primary transport mechanism in many circumstances for particles less than 0.1 μm in size (Fuchs, 1964). Although both convective and diffusive transport contribute to the motion of a pollutant, at a solid (non-porous) surface the velocity components are zero and the deposition flux is simply equal to the rate of diffusion to that surface. Written in terms of activity concentration, Fick's law can be applied at the surface to obtain the activity deposition flux, j:

$$j = D\,(dA/dn)\Big|_{surface} \tag{3}$$

where n is the distance measured normal to the wall. Equation (3) is written with the convention that j is positive towards the wall, when n is measured positive away from the wall. Deposition can also be parameterized in terms of a concentration difference driving potential, and a mass transfer coefficient u, (analogous to the convective coefficient used in heat transfer theory):

$$j = u\,(A_c - A_s) = u\,A_c \tag{4}$$

$$u = j / A_c = (D/A_c)\,(dA/dn)\Big|_{surface} \tag{5}$$

where $A_c$ is the concentration in the core of the enclosure, or far away from the boundary layer, and $A_s$ is the surface concentration, equal to zero. The mass transfer coefficient, u, has units of length/time and is called the "deposition velocity", commonly expressed in units of (cm/sec). It is defined as the flux density per unit core concentration, and can be considered the effective velocity of particles migrating to a surface.

Equation (5) represents the local deposition velocity at a point along a surface. One can also calculate the average deposition velocity, <u>, and relate it to the deposition rate constant, q, used in the uniform-mixing model. The rate constant q is essentially a volumetric reaction rate and a measure of the average probability that particles will reach known boundaries (Fuchs, 1964). In the uniform-mixing model, q is used to express the total rate of activity deposition, J:

$$J = q\, A_{avg}\, V \tag{6}$$

Equation (3) can also be integrated over the entire space to obtain:

$$J = \int D\,(dA/dn)\, dS = \langle j \rangle S = \langle u \rangle A_c\, S \tag{7}$$

For a large enclosure, $A_{avg}$ is approximately equal to $A_C$. Equation (6) and (7) can then be combined to give:

$$q = \langle u \rangle S/V \tag{8}$$

This equation implies that the room is well-stirred. If one assumes that all surfaces are equally effective for deposition, then equation (8) can be used to apply calculations of <u> to different situations. While the deposition ra constant q is used as input to the uniformly-mixed model, it is more appropriate to compare research results using the deposition velocity u, since u is more descriptive of deposition as a surface phenomenon.

*3.2 Deposition of Radon Progeny*

Experimental measurements are often in terms of total (free plus attached) progeny concentrations and total deposition rates, $q_i$. However, the deposition rates (or velocities) of the free and attached radon progeny have to be determined independently due to their differences in diffusivity and concentration profiles. The total rate of activity deposition, for each decay product i, is simply the sum of the free and attached contributions:

$$J_i = J_i^f + J_i^a = q_i^f\, A_i^f\, V + q_i^a\, A_i^a\, V \tag{9}$$

The individual quantities, $q_i^f$ and $q_i^a$, are connected to the total deposition rate through the free fraction, $f_i$. For each decay product i, the free fraction $f_i$ is defined as the ratio of free to total progeny activity concentration:

$$f_i = A_i^f / (A_i^f + A_i^a) = A_i^f / A_i \tag{10}$$

where A in equations (9) and (10) represents average activity concentration. The total deposition rate constant is obtained by combining equations (6), (9), and (10):

$$q_i = f_i\, q_i^f + (1-f_i)\, q_i^a \tag{11}$$

RADTRAN can be used to obtain values of deposition velocities and overall deposition rate constants for a specified set of environmental conditions. In summary, the steps used in RADTRAN for examining radon progeny deposition are: (*i*) solve for the spatial activity concentration distributions in the space, $A^f$ and $A^a$; (*ii*) calculate local activity flux, $j^f$ and $j^a$, along each surface using equation (3); (*iii*) integrate the local flux over all surfaces to determine the total rates of deposition in the space, $J^f$ and $J^a$; (*iv*) calculate local deposition velocities, $u^f$ and $u^a$, and average deposition velocities, $\langle u^f \rangle$ and $\langle u^a \rangle$, using equations (5) and (7), respectively; (*v*) calculate overall deposition rate constants, $q^f$ and $q^a$, using equation (8); (*vi*) calculate the free fraction, f, using average concentrations in equation (10); and (*vii*) calculate the total deposition rate, q, using equation (11).

### *3.3 Other Deposition Processes*

As a necessary simplification in the initial development and application of RADTRAN, several deposition mechanisms were neglected. These mechanisms are described briefly below, with references for more detailed explanations.

Deposition rates in a turbulent flow are much higher than those in laminar conditions. The process of turbulent deposition is extremely complex,. Among the difficulties in theoretically predicting turbulent deposition rates are these: determining the functional form of the eddy viscosity (which varies throughout the regimes of a turbulent flow); accounting for the extent to which particles follow the turbulent fluctuations (expressed by a relationship between the eddy diffusivity and eddy viscosity); and incorporating the rate of re-entrainment of the deposited particles (which is likely to occur when the turbulent flow velocity is high).

The magnitude of deposition due to gravitational settling increases rapidly with particle size, and is described by the particle's terminal settling velocity. Although gravitational settling onto horizontal surfaces is negligible for the free progeny, it is significant for the attached progeny and dominates other transport mechanisms for particle diameters greater than 0.3 μm (Nazaroff & Cass, 1987).

An example of inertial impaction is when a surface causes an airstream to turn, and particles with sufficient inertia are unable to follow the streamlines and impact on the surface. The potential for inertial deposition increases with particle diameter and air velocity and is insignificant at the low velocities prevalent indoors, particularly for the smaller free progeny (Hinds, 1982; Nazaroff & Cass, 1987).

Most particles carry some electric charge and will experience an electrostatic force in the vicinity of charged surfaces. This force depends on the magnitude of the particle charge, and the strength of the electric field in the space around the charged surface. A general discussion of electrostatic forces on particles is given by Hinds (1982) and McMurry & Rader (1985), and a simplified approach for examining electrophoretic deposition in enclosures is presented by van de Vate (1980). It is difficult to assess the relative importance of electrophoresis, given the lack of available data on electric field strengths near room surfaces (Nazaroff & Cass, 1987).

Thermophoretic deposition is caused by thermal forces on the particle resulting from temperature gradients in the air, creating a net force in the direction of cooler temperature. van de Vate (1980) examined thermophoretic deposition in enclosures, and Nazaroff & Cass (1987) used scale analysis and numerical analysis based on a similarity transformation to investigate particle deposition due to convection, molecular diffusion, and thermophoresis in a natural convection boundary layer flow. Their work showed that the effect of thermophoresis is relatively small for the size of free radon progeny, but can be substantial for particles (and attached progeny) larger than 0.1 μm.

RADTRAN does not currently account for any of the deposition mechanisms described above. Although gravitational settling and thermophoresis may have a non-negligible impact on attached progeny deposition, the primary focus of the initial RADTRAN simulations was the investigation of free progeny deposition. Including the complex processes of electrostatic and turbulent deposition would be desirable for further development of the model.

## 4.0 FLOW CHARACTERIZATION

Understanding the airborne transport of pollutants requires detailed information about the air flow patterns in the space. Air movement in a building can be generated in a number of ways: infiltration, natural ventilation, mechanical ventilation, buoyancy-driven natural convection, or the movement of people and objects. The air flow patterns are typically due to a combination of several influences, and the characterization of these flows is difficult. Simulations reported here examined laminar buoyancy-driven recirculating enclosure flows, free and forced convection boundary layer flows along isolated surfaces, and diffusion-only conditions. Natural convection flows represent conditions where there are relatively insignificant sources of forced air flows (e.g., no open windows or forced air heating or cooling systems), and surface temperatures that vary from those of the room air (e.g., a room with perimeter walls or windows). The forced convection flow might represents conditions driven by a mechanical ventilation system where the supply air is delivered parallel to a surface. The diffusion-only analysis might represent no-flow stable conditions, such as a stratified enclosure with a warm ceiling and cool floor. The diffusion model also serves as a base case to compare the relative effects of air movement on pollutant deposition.

For the complex recirculating flows, RADTRAN uses velocity data generated from a separate model of air movement in buildings. For the simple one-directional boundary layer flows, the model calculates the velocity profiles using integral methods of solution of the boundary layer form of the Navier-Stokes equations. A later section describes the relationships generated from the diffusion-only model in more detail.

### *4.1 Buoyancy-Driven Enclosure Flows*

Buoyancy-induced fluid motion, commonly referred to as "natural convection", is the result of gravitational body forces acting on the fluid. These forces are due to density differences arising from temperature gradients in the space. There will generally be some degree of natural convection due to temperature differences within the space, although the relative strengths of natural and forced convective flow will depend on factors such as the magnitude of the temperature differences (due to heat distribution and solar gain) and the source of the forced air flow.

The motion of the fluid is described by the Navier-Stokes equations (Bird *et al.*, 1960; Spalding, 1963). These are non-linear, partial differential equations representing the laws of conservation of mass, momentum, and energy applied to a fluid element. The momentum and energy equations are coupled through the body force term; consequently, the velocity field depends on the temperature distribution. Assuming that pollutant concentrations are not high enough to affect the air viscosity and velocity profiles, the Navier-Stokes equations are decoupled from the mass-transport equation, and the velocity fields can be determined independently of the concentration distributions. Two important dimensionless parameters characterizing natural convection flow in an enclosure are the Grashof number ($Gr = g \beta \Delta T L^3/v^2$), and the Rayleigh number ($Ra = Pr\ Gr$) (Bird et al., 1960; Schlichting, 1979).

For input to RADTRAN, data representing the velocity field in an enclosure were obtained from a con-

vection model developed by Gadgil (1980), based on a numerical discretization of the Navier-Stokes equations for laminar conditions. This two-dimensional convection model simulates both natural and forced convection, for any combination of rectangular obstacles, openings, and velocity or heat sources and sinks in a rectangular shaped enclosure, at Rayleigh numbers up to $10^{10}$ (Gadgil 1980). Velocity fields for the initial simulations of RADTRAN were calculated for a two-dimensional square enclosure, with boundary conditions corresponding to isothermal hot and cold walls and adiabatic floor and ceiling. A schematic drawing of streamlines in this flow is shown in Figure 2.

*4.2 Boundary Layer Flows*

In addition to enclosure flows, pollutant transport was also simulated for simpler boundary layer flows. Boundary layer theory can be applied both to the Navier-Stokes equations to obtain velocity profiles, and also to the mass-transport equations for radon progeny to obtain concentration profiles (Bird et al., 1960; Schlichting, 1979). The velocity in a boundary layer flow is predominantly in one direction without recirculation. The flow at one point is independent of the downstream behavior, and convection always dominates diffusion in this streamwise direction. Changes in pollutant concentration occur essentially over a narrow layer near the surface, which is thin relative to the dimensions of the surface.

For many enclosure flows, specific regions of the flow can often be represented by simpler boundary layer flows. An example of this is the simple enclosure flow that was investigated in these simulations. Velocity profiles showed that the flow along the walls can be approximated by a boundary layer free convection flow along an isothermal single surface within quiescent surroundings, unbounded by other surfaces; and the flow along the floor and ceiling can roughly be approximated by a boundary layer forced convection flow along a horizontal flat plate with an imposed freestream velocity (Schiller, 1984). Schematic diagrams of velocity profiles in these free and forced convection boundary layer flows are shown in Figures 3 and 4, respectively.

A significant consequence of the boundary layer approximation is that it changes the character of the transport equation from an elliptic to a parabolic form. An elliptic equation is a boundary-value problem and can only be solved by specifying the boundary conditions on a complete contour enclosing the region. A parabolic equation, on the other hand, is a mixed initial- and boundary-value problem. Conditions need only be specified at one x-position, where x represents the streamwise direction. Computer solutions are then relatively easier because x is now a marching variable; the profile can be initialized at x=0 and the solution then "marches" down the plate in the direction of the flow (Patankar, 1980).

A boundary layer flow analysis is advantageous compared to a full enclosure flow for several reasons. The solution at a particular point is independent of the behavior downstream; consequently, the iterative procedure used for recirculating flows is not necessary and storage requirements and computing costs are substantially less. The grid only needs to be extended out to the edge of the boundary layer, so one can get more detailed information near the wall by incorporating a much finer grid in this region than is possible for an entire enclosure. Overall, it is faster and less expensive to use a boundary layer analysis, particularly for the many simulations required for parametric sensitivity studies.

## 5.0 SIMPLIFIED DIFFUSION MODEL

A simplified form of the mass-transport model is a one-dimensional diffusion model in which convective transport near the wall is neglected entirely. This is commonly known as the film model, and it assumes that the species diffuses through a stagnant film near the surface. The thickness of this film is defined such that beyond its outer edge the fluid is well-mixed and concentration gradients are negligible (Bird et al., 1960). The mathematical formulation of this model is essentially an equation describing one-dimensional diffusion of a chemically reactive species, and can be solved exactly. (It should be noted that the mathematical concept of a boundary layer does not apply in a one-dimensional model, thus the term "film thickness" or "wall region" is more appropriate for this case).

An advantage of applying this model to the free and attached radon decay products is that it results in analytic expressions for the concentration distributions and mass-transfer coefficients, or deposition velocities, $u^f$ and $u^a$. Although the model may not accurately represent room conditions, it provides a simple physical picture and much of the insight gained from studying its results can also be applied to more complex systems. Consequently, the mathematical formulations serve as a good starting point for illustrating some of the physical concepts governing the behavior of indoor radon decay products. The expressions developed in this section will be useful for interpreting results generated from the more complex model including convective transport.

The complete solutions to the one-dimensional diffusion equations are presented in the Appendix. The equations describing concentration distributions can be manipulated to solve for the free and attached deposition velocities in stagnant conditions. The resulting expressions illustrate the complexities of the dependence of $u^f$ and $u^a$ on the physical parameters and, most importantly, the potential differences between decay products. These relationships are discussed in more detail in a companion paper describing the results of parametric studies using RADTRAN (Schiller and Revzan, 1989).

The final expressions for $u^f$ and $u^a$ for the first decay product, $^{218}Po$ ($i = 1$), are relatively simple and are presented here for reference and discussion:

$$u_1^f = D^f / d_1^f \qquad u_1^a = D^a / (d_1^f + d_1^a) \tag{12}$$

where $d^f$ and $d^a$ are the free and attached progeny "diffusion lengths" defined by:

$$d_1^f = [\, D^f / (\lambda_1 + X) \,]^{1/2} \qquad d_1^a = [\, D^a / \lambda_1 \,]^{1/2} \tag{13}$$

Substituting equations (13) into (12), and noting that $d_f >> d_a$, $u_1^f$ and $u_1^a$ can be written as:

$$u_1^f = [\, D^f (\lambda_1 + X) \,]^{1/2} \tag{14a}$$

$$u_1^a = D^a [\, (\lambda_1 + X) / D^f \,]^{1/2} = [\, D^a/D^f \,]^{1/2} \cdot [\, D^a (\lambda_1 + X) \,]^{1/2} \tag{14b}$$

An effective concentration film thickness, b, can be defined by assuming a linear concentration profile with a slope equal to the gradient at the wall. The deposition velocities can then be expressed as:

$$u_1^f = D^f / b_1^f \qquad u_1^a = D^a / b_1^a \tag{15}$$

Combining equations (12) and (15), the effect film thicknesses for one-dimensional diffusion are related to the dif-

fusion lengths by:

$$b_1^f = d_1^f \qquad b_1^a = d_1^f + d_1^a \tag{16}$$

Since $d^f >> d^a$, these equations imply that the deposition velocity of attached $^{218}Po$ is much smaller than for particles of equal size, when convection is neglected. A comparison of particle deposition and attached $^{218}Po$ deposition is presented by Schiller and Revzan (1989).

*5.1 Factors Influencing Deposition Rates*

Equations (14) express the functional dependence of $u_1^f$ and $u_1^a$ on $D^f$, $D^a$, $\lambda$, and $X$, for $^{218}Po$ in stagnant conditions. The expressions are simple, yet they are indicative of important physical concepts which cannot be illustrated from the uniformly-mixed model or existing experimental measurements. For the simplified case of diffusion-only, the concentration distribution of the attached progeny is strongly determined by that of its source, the free progeny. Consequently, the attached progeny concentration profile, and the corresponding wall region thickness, $b^a$, will actually depend on both the free and attached diffusion lengths, $d^f$ and $d^a$. One implication of this result is that $u^a$ depends not only on attached diffusivity, $D^a$, but also on the physical nature of the free progeny, as described by $D^f$. Equation (14b) also demonstrates that the value of $u^a$ is greatly reduced compared with the deposition velocity of equivalently sized particles, by a factor of $[D^a/D^f]^{1/2}$.

This same concept can be applied to all the decay products, and the equations are presented in the Appendix. The concentration profile for each decay product is determined not only from its respective diffusion coefficients, but is strongly dependent on the source distribution. Since each of the decay products is generated from a different source, it is natural to assume that there will also be variations between their deposition velocities. The equations in the Appendix indicate how the deposition velocities differ among the decay products for stagnant conditions.

## 6.0 MODEL VALIDATION

Initial simulations of RADTRAN examined the influence of key parameters on deposition velocities of the first three radon progeny, with a particular emphasis on the free mode of the first decay product, $^{218}Po$. In the parametric studies, $D^f$ and $X$ (as a function of N) were varied over ranges representative of experimental findings for realistic room conditions. Both free and forced convection were varied over the laminar flow regime. A second paper (Schiller and Revzan, 1989) describes in more detail the influence of these parameters on deposition. The range of deposition velocities found in these parametric studies are compared here to experimental findings.

### *6.1 Existing Experimental Studies*

Air flow conditions have varied considerably in experimental studies of radon deposition. Measurements have been made in occupied buildings, experimental rooms, small chambers, wind tunnels, and diffusion tubes. Although conditions in the small chambers, wind tunnels, and diffusion tubes are easiest to control and quantify, these are probably least representative of realistic conditions in buildings. In particular, the wind tunnel studies have predominantly been used to examine outdoor aerosol deposition, and the air speeds investigated are often much higher than the magnitudes likely to be seen in indoor spaces.

To validate the model as a predictive tool, it is necessary to compare the predictions with experiments in which the conditions are similar to the simplified flows simulated in the model. These include near-stagnant conditions or laminar flows. Unfortunately, reports of experimental work typically give only qualitative descriptions of the air motion in the test spaces, if any discussion is presented at all. Experiments have included relatively still conditions (George et al., 1983; Knutson et al., 1983; Rudnick et al., 1983; Vanmarke, 1984; Bigu, 1985; McLaughlin et al., 1985); natural convective flow (Scott, 1983); laminar and turbulent controlled flows (wind tunnels and tube flows) (Sehmel, 1971; Clough, 1973; Pörstendorfer, 1983); and conditions in which air cleaner fans or mixing fans were used, or flows were stated as being turbulent (Rudnick et al., 1983; Sextro et al., 1984; Bigu, 1985). There have only been a few cases where air velocities were actually measured (Sehmel, 1971; Scott, 1983). In general, flow conditions in the experiments have not been well characterized. Table 1 presents a summary of the conditions and results of representative experiments used for comparison to RADTRAN's predictions.

### *6.2 Model Predictions*

The parameters varied in the RADTRAN simulations were $D^f$, $X$, and air motion. Values of $D^f$ were varied over an order of magnitude, 0.01 - 0.10 $cm^2/sec$, encompassing the range found by the majority of researchers and centering around the commonly used value of 0.054 $cm^2/sec$ (Chamberlain et al., 1956; Busigin et al., 1981; Bruno, 1983; Knutson et al., 1983; Phillips et al., 1988). The range of $X$ (0-250 $hr^{-1}$) corresponds to a particle concentration up to N = 60,000 particles/$cm^3$ (assuming a mean particle diameter of 0.1 μm, and a corresponding attachment coefficient of $4.3 \times 10^{-3}$ $hr^{-1}$/(particles/$cm^3$)). This extends beyond the range typically found indoors, except in the case of very heavy smoking.

The free stream velocity in a forced-convection boundary layer flow was varied from 1-100 cm/sec, on a horizontal plate 3 m long. The upper velocity of 100 cm/sec corresponds to a Reynold's number of $2 \times 10^5$. This is below the critical number $Re_{cr} = 3 \times 10^5$, at which transition to turbulence occurs (Knudsen & Katz, 1958; Schlichting, 1979). A free-convection boundary layer flow on a vertical hot plate was also examined, for Grashof numbers of $3 \times 10^9$ and $3 \times 10^{10}$. (This corresponds to Rayleigh numbers of $2 \times 10^9$ and $2 \times 10^{10}$, since Pr = 0.7 for air). These two numbers represent the transition to turbulence for an isolated surface, as quoted by various sources. The critical value of $Ra_{cr} = Gr\ Pr = 10^9$ is given by Bird et al. (1960) and Schlichting (1979), while the value of $Ra_{cr} = 10^{10}$ is given by Kaplan (1963), Gadgil (1980), Nansteel & Greif (1981), and Bohn et al. (1983). For flow inside an enclosure, transition to turbulence occurs at higher critical Rayleigh numbers than for isolated surfaces (Ruberg,

1978; Nansteel & Greif, 1981; and Bohn et al., 1983). An enclosure of 3 m x 3 m with a buoyancy-driven recirculating flow (isothermal hot and cold walls, adiabatic floor and ceiling) was simulated, characterized by Grashof numbers of $3x10^9$ and $3x10^{10}$. The simplified case of one-dimensional diffusion, was also simulated.

Figure 5 presents a summary of values of $u^f$ and $u^a$ obtained by researchers, and the range of values predicted by the mass-transport model from the parametric studies. Of the experiments shown, those with flow conditions most similar to the ones simulated with RADTRAN include: George et al. (1983) in a small 1.9 $m^3$ chamber with minimal air flow, Rudnick (1983) in a 78 $m^3$ experimental room without mixing fans, Vanmarcke (1984) in a small one $m^3$ chamber with near-stagnant conditions, and Bigu (1985) in a large 26$m^3$ chamber with still air conditions.. Because the geometry and value of S/V in these experiments varied considerably (1.9 - 6.0 $m^{-1}$), the comparison is made in terms of deposition velocity rather than the geometry-dependent deposition rate constant.

Table 1 and Figure 5 show that results from experiments with laminar or still air flow conditions (George et al., 1983; Rudnick et al., 1983; Vanmarke, 1984; and Bigu, 1985) are contained within the range of 0.014 - 0.079 cm/sec predicted by RADTRAN for $u^f$. This is considered a rough comparison, given the lack of precise information regarding the flow conditions of the experiments. Experiments by McLaughlin et al. (1985) were also conducted under still air conditions and compared will with RADTRAN, although tests were done in a small cylindrical chamber where both the size and geometry was significantly different than conditions simulated by RADTRAN. Recent experiments by Pörstendorfer (1983, 1985) also compared well. Results of the parametric studies suggest that experimental values of $u^f$ greater than approximately 0.08 cm/sec cannot be accounted for by laminar convective diffusion. Higher values are most likely due to deposition mechanisms not simulated, such as electrostatic attraction, or turbulent diffusion.

Among these experiments, only those of George and Knutson reported a value of $u^a$. They estimated $u^a \approx 0.5\text{-}1.0x10^{-3}$ cm/sec, for tests where the geometric mean particle diameter varied in the range 0.06-0.15 μm. Values of $u^a$ predicted from RADTRAN were at least an order of magnitude lower than this, ranging from $\approx 0.4\text{-}0.7x10^{-4}$ cm/sec. This is most likely due to that fact that only deposition by molecular diffusion was accounted for in the simulations. Because of their larger size, attached progeny are much more sensitive to inertial, gravitational, and thermophoretic effects, and these need to be accounted for. Further studies of deposition due to electrostatic forces may also account for these differences. While the uncertainty in the predicted values of $u^a$ is high, the total deposition rate of radon progeny is almost entirely influenced by $u^f$ except for very high particle concentrations . Consequently, it is not expected that these low values of $u^a$ will contribute to large uncertainties in RADTRAN's predictions of overall room concentrations.

## 7.0 CONCLUSIONS

A mass-transport model, RADTRAN, has been developed based on mass conservation and transport laws governing the movement of reactive components in specified laminar flow conditions. Equations for the

concentrations of each of the first three radon progeny, in both the free and attached modes, are written in two-dimensional form, and their solution is based on an approximate numerical technique. Deposition is treated as a surface reaction represented by a boundary condition. RADTRAN is able to account for variability in source distributions and transport mechanisms, and their influence on concentration distributions and deposition rates. The mass-transport model offers many advantages over existing indoor radon models by providing a more realistic basis for understanding radon progeny behavior.

In simulations using RADTRAN, several flow conditions have been examined: buoyancy-driven recirculating enclosure flows, free and forced-convection boundary layer flows, and one-dimensional diffusion. Free progeny diffusivity, Df, and attachment rate, X, were varied over representative ranges. For these conditions, RADTRAN calculated free deposition velocities of $u^f$ = 0.014 - 0.079 cm/sec, for $^{218}Po$. This range is in rough agreement with findings from experiments conducted in flow conditions similar to the simplified flows used in RADTRAN.

RADTRAN is based on fundamental laws of physics, and the approach can also be applied to other pollutants simply by appropriately changing the transformation rates and boundary conditions. For example, the modeling approach can be used to investigate the transport and distribution of a pollutant within a space for a specified source distribution. A point source might represent combustion products from a stove, heater, or cigarette, and a line or area source might represent the emanation of pollutants from building materials. The fundamental basis of this model enables the method to be used for quantitatively examining the behavior of pollutants for which surface interactions are particularly important. One example of such a pollutant is formaldehyde, where the walls can act as both a source and a sink. However, the boundary conditions for formaldehyde or volatile organic compounds are quite complex and difficult to describe mathematically. A model would have to include a detailed description of the adsorption on, desorption from, and diffusion through the surface materials, and the dependence of these mechanisms on temperature and humidity conditions.

The applicability of the mass-transport model is primarily limited by the ability to simulate flow conditions representative of realistic conditions. The air flows that typically exist in real buildings are complex and difficult to accurately characterize through either measurements or theoretical simulations. Although laminar flow is admittedly a simplification of realistic conditions, this approach represents a necessary first step in attempting to characterize the effects of air motion on radon progeny transport and deposition. RADTRAN provides a theoretical framework for further studies concerning the general behavior and interactions of indoor radon and its decay products, and provides the basis from which a more comprehensive and realistic model of indoor air quality can be developed.

## 9.0 ACKNOWLEDGEMENTS

This work was supported by the Director, Office of Energy Research, Office of Health and Environmental Research, Pollutant Characterization and Saftey Research Division, and by the Assistant Secretary for Conservation and Renewable Energy, Office of Buildings and Community Systems, Building Systems Division, of

the U.S. Department of Energy under Contract No. DE-AC03-76SF00098. Sincere thanks are extended to Ken Revzan and Rich Sextro for their helpful discussions and suggestions, and to Bill Nazaroff for his invaluable literary critique and his endless supply of patience and encouragement.

## 9.0 REFERENCES

Bird, R.B., W.E. Stewart, and E.N. Lightfoot, 1960, Transport Phenomena, John Wiley & Sons, New York.

Bohn, M., D. Olson, and A. Kirkpatrick, 1983, "Experimental Study of Three-Dimensional Natural Convection at High Rayleigh Numbers", ASME Paper No. 83-HT-12.

Browne, E., and R.B. Firestone, 1986, Table of Radioactive Isotopes, V.S. Shirley (ed.), John Wiley & Sons, New York.

Bruno, Ronald C., 1983, "Verifying a model of radon decay product behavior indoors", Health Physics, Vol.45, No.2, pp.471-480.

Busigin, A., A.W. van der Vooren, J.C. Babcock, and C.R. Phillips, 1981, "The nature of unattached RaA (Po-218) particles", Health Physics, Vol.40, pp.333-343.

Chamberlain, A.C., and E.D. Dyson, 1956, "The dose to the trachea and bronchi from the decay products of radon and thoron", Br. J. Radiol., 29, pp.317-325.

Clough, W.S., 1973, "Transport of particles to surfaces", J. of Aerosol Science, Vol.4, pp.227-234.

Fuchs, N.A., 1964, The Mechanics of Aerosols, Pergamon Press, Oxford.

Gadgil, A.J., 1980, "On convective heat transfer in building energy analysis", Ph.D. Thesis, Department of Physics, University of California, Berkeley. Also published as Report #LBL-10900, Lawrence Berkeley Laboratory, California.

George, A.C., E.O. Knutson, and K.W. Tu, 1983, "Radon daughter plateout - I: Measurements", Health Physics, Vol.45, No.2, pp.439-444.

Hinds, W.C., 1982, Aerosol Technology, John Wiley & Sons, New York.

Jacobi, W., 1972, "Activity and potential alpha-energy of (222)radon- and (220)radon-daughters in different air atmospheres", Health Physics, Vol.22, pp.441-450.

Kaplan, I., 1963, Nuclear Physics, 2nd ed., Cambridge Mass., Addison-Wesley Publishing Co.

Knudsen, J.G., and D.L. Katz, 1958, Fluid Dynamics and Heat Transfer, Engineering Research Institute, University of Michigan Press.

Knutson, E.O., A.C. George, J.J. Frey, and B.R. Koh, 1983, "Radon daughter plateout - II: Prediction model", Health Physics, Vol.45, No.2, pp.445-452.

McMurry, P.H., and D.J. Rader, 1985, "Aerosol wall losses in electrically charged chambers," Aerosol Science and Technology, 4, pp.249-268.

Mercer, T.T., 1976, "The effect of particle size on the escape of recoiling RaB atoms from particulate surfaces", Health Physics, Vol. 31, pp.173-175.

Nansteel, M., and R. Greif, 1981, "Natural Convection in Undivided and Partially Divided Rectangular Enclosures", ASME Journal of Heat Transfer, Vol. 103, pp.623-629.

Nazaroff, W.W., and K.Y.Teichman, "Indoor Radon: Exploring Policy Options for Controlling Human Exposures", Report #LBL-27148, Lawrence Berkeley Laboratory, California.

Nazaroff, W.W., and A.V. Nero, eds., 1988, Radon and Its Decay Products in Indoor Air, John Wiley & Sons, Inc.

Nazaroff, W.W., and G.R. Cass, 1987, "Particle Deposition from a Natural Convection Flow onto a Vertical

Isothermal Flat Plate," J. of Aerosol Science, Vol. 18, No.4, pp.445-455.

Nero, A.V., 1988, "Controlling Indoor Air Pollution," Scientific American, Vol. 258, No. 5, pp.42-48.

Patankar, S.V., 1980, Numerical Heat Transfer and Fluid Flow, McGraw-Hill Book Co., New York.

Phillips, C.R., A. Kahn, and H.M.Y. Leung, 1988, "The Nature and Determination of the Unattached Fraction of Radon and Thoron Progeny," Radon and Its Decay Products in Indoor Air, W.W. Nazaroff and A.V. Nero, eds., John Wiley & Sons, Inc., pp.203-256.

Pörstendorfer, J., 1984, "Behaviour of radon daughter products in indoor air", Radiation Protection Dosimetry, Vol.7, No.1-4, pp.107-113.

Pörstendorfer, J., A. Wicke, and A. Schraub, 1978a, "The influence of exhalation, ventilation and deposition processes upon the concentration of radon (Rn-222), thoron (Rn-220) and their decay products in room air", Health Physics, Vol.34 (May), pp.465-473.

Pörstendorfer, J., and T.T. Mercer, 1978b, "Influence of nuclei concentration and humidity on the attachment rate of atoms in the atmosphere", Atmos. Environ., Vol. 12, pp.2223-2228.

Raes, F., A. Janssens, and H. Vanmarcke, 1985, "A Closer Look at the Behaviour of Radioactive Decay Products in Air," The Science of the Total Environment, Vol. 45, pp.205-218.

Raes, F., A. Janssens, and H. Vanmarcke, 1987, "A Model for Size Distributions of Radon Decay Products in Realistic Environments," Radon and Its Decay Products: Occurence, Properties, and Health Effects, P.K. Hopke (ed.), ACS Symposium Series 331, American Chemical Society, Washington D.C., pp.324-339.

Ruberg, K., 1987, M.S. Thesis, Massachusetts Institute of Technology.

Rudnick, S.N., W.C. Hinds, E.F. Maher, and M.W. First, 1983, "Effect of plateout, air motion and dust removal on radon decay product concentration in a simulated residence", Health Physics, Vol.45, No.2, pp.463-470.

Schiller, G.E., and K.L. Revzan, 1989, "Transport and Deposition of Indoor Radon Decay Products: Part 2 - Influence of Environmental Conditions". *Submitted to Atmospheric Environment.*

Schiller, G.E., 1984, "A Theoretical Convective Transport Model of Indoor Radon Decay Products," Ph.D. Thesis, University of California, Berkeley. Also published as Report #LBL-20096, Lawrence Berkeley Laboratory, California.

Schlichting, H., 1979, Boundary-Layer Theory, 7th ed., McGraw-Hill.

Scott, A.G., 1983, "Radon daughter deposition velocities from field measurements", Health Physics, Vol.45, No.2, pp.481-485.

Sehmel, G.A., 1970, "Particle deposition from turbulent air flow", Journal of Geophysical Research, Vol.75, No.9, pp.1766-1781.

Sehmel, G.A., 1971, "Particle diffusivities and deposition velocities over a horizontal smooth surface", Journal of Colloid and Interface Science, Vol.37, No.4, pp.891-906.

Spalding, D.B., 1963, Convective Mass Transfer, McGraw-Hill Book Co., New York.

van de Vate, Joh. F., 1980, "Investigations into the dynamics of aerosols in enclosures as used for air pollution studies", Research Report, Netherlands Energy Research Foundation.

Vanmarcke, H., 1984, Nuclear Physics Laboratory, Belgium, personal communication.

# RADON DECAY CHAIN

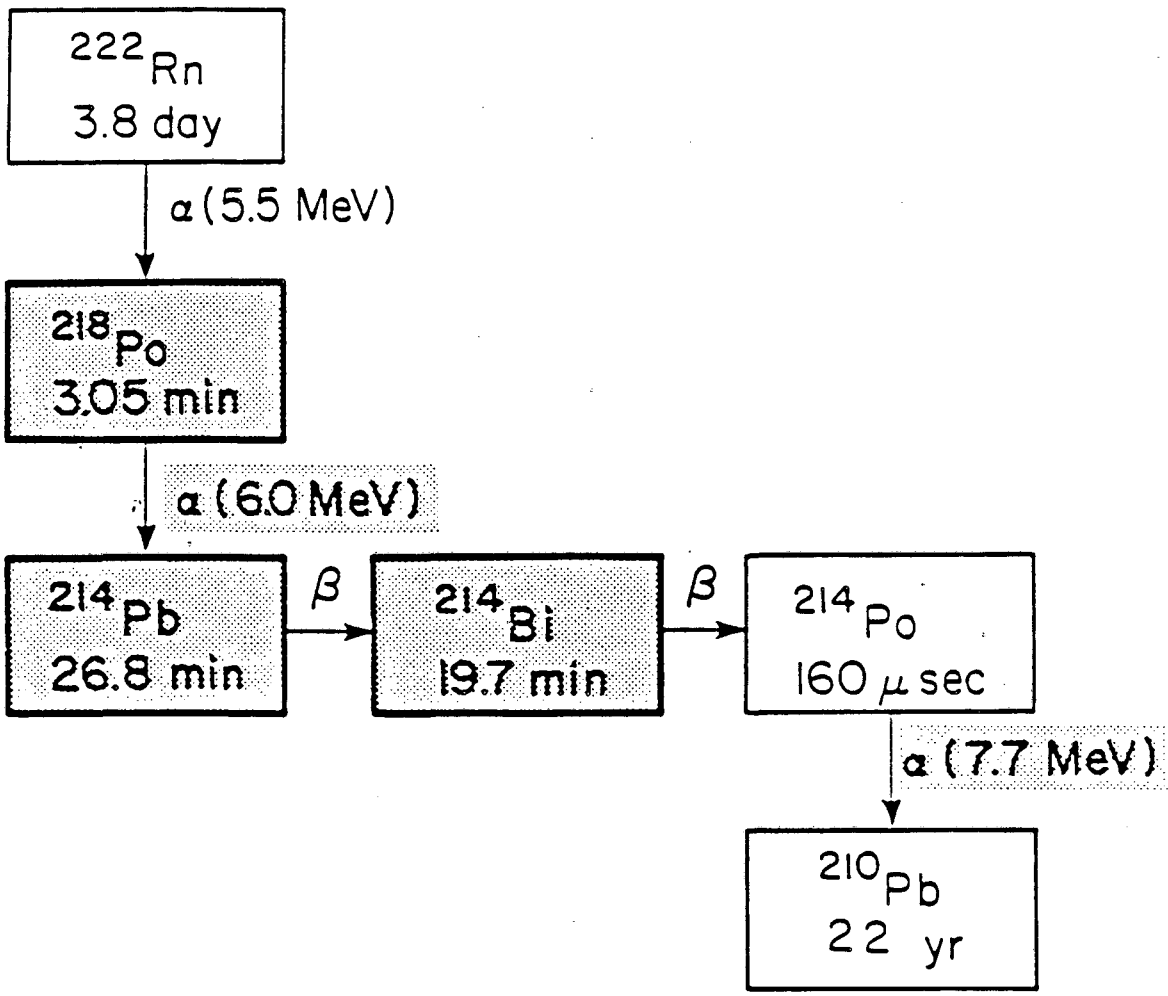


Figure 1. The radon and radon progeny decay chain, with the corresponding half-lives and principal type of radiation associated with each. The shaded isotopes are those of primary biological concern due to inhalation and subsequent alpha decay. The half-lives shown in the figure are the numbers used in RADTRAN. Browne and Firestone (1986) provide updated values.

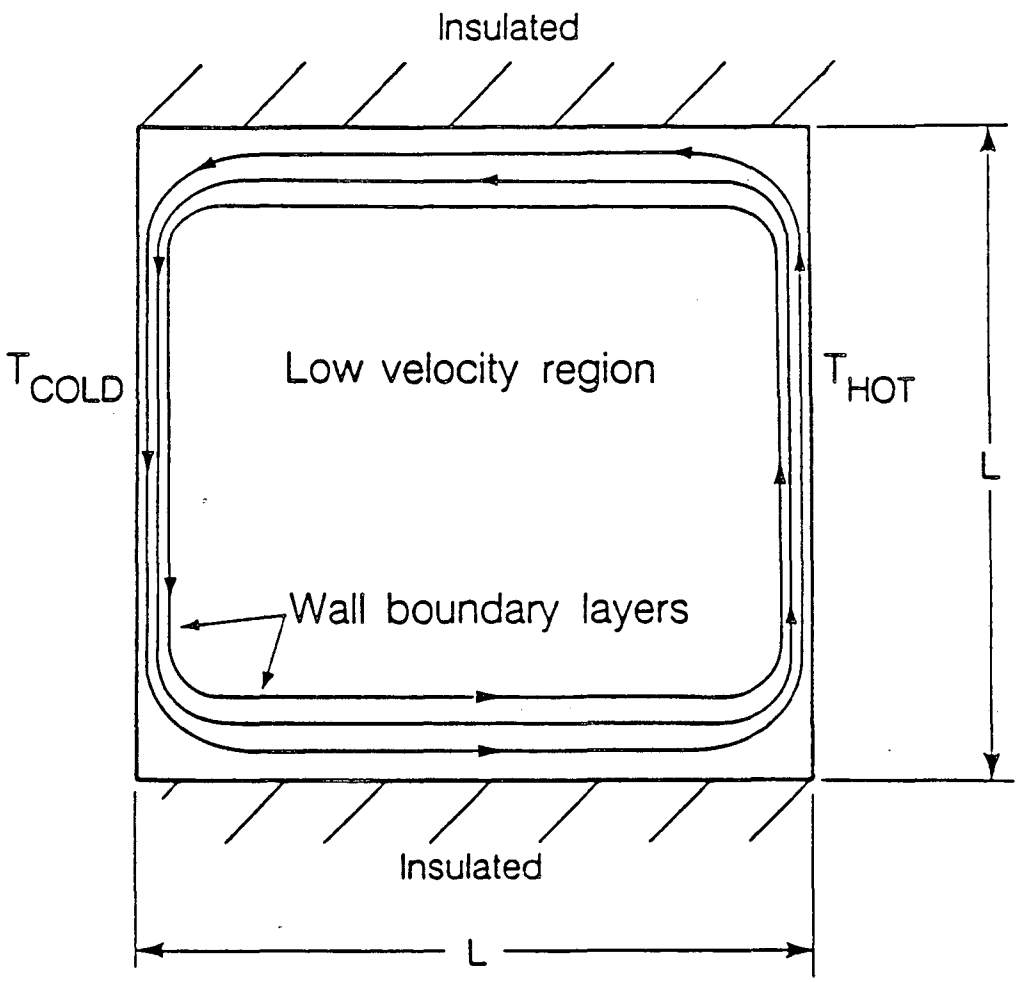


Schematic Diagram of a Buoyancy-driven Enclosure Flow

Figure 2. Schematic diagram of streamlines, illustrating the velocity field in a simplified buoyancy-driven flow. Velocities are highest along the isothermal walls, as indicated by the streamlines being closer together.

Schematic Diagram of a Free Convection Boundary Layer Flow

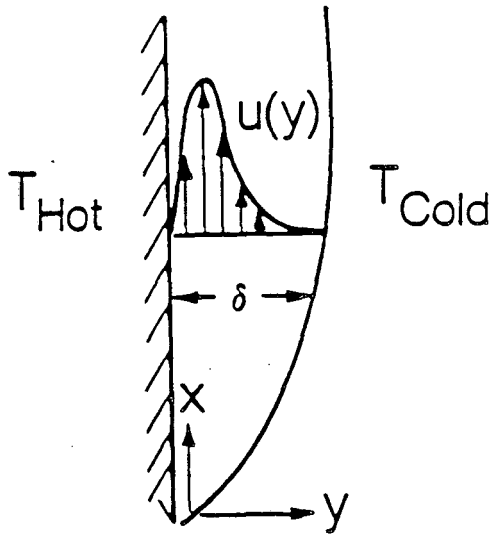


Figure 3. Representative velocity profile, u(y), of a free convection boundary layer flow along a hot, isothermal vertical surface within cooler, quiescent surroundings, unbounded by other surfaces.

Schematic Diagram of a Forced Convection Boundary Layer Flow

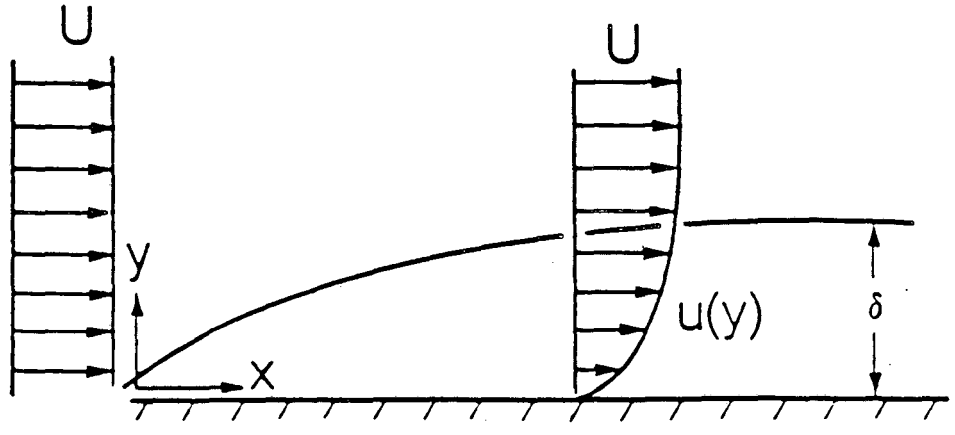


Figure 4. Representative velocity profile, u(y), of a forced convection boundary layer flow along a horizontal flat plate with an imposed freestream velocity, U.

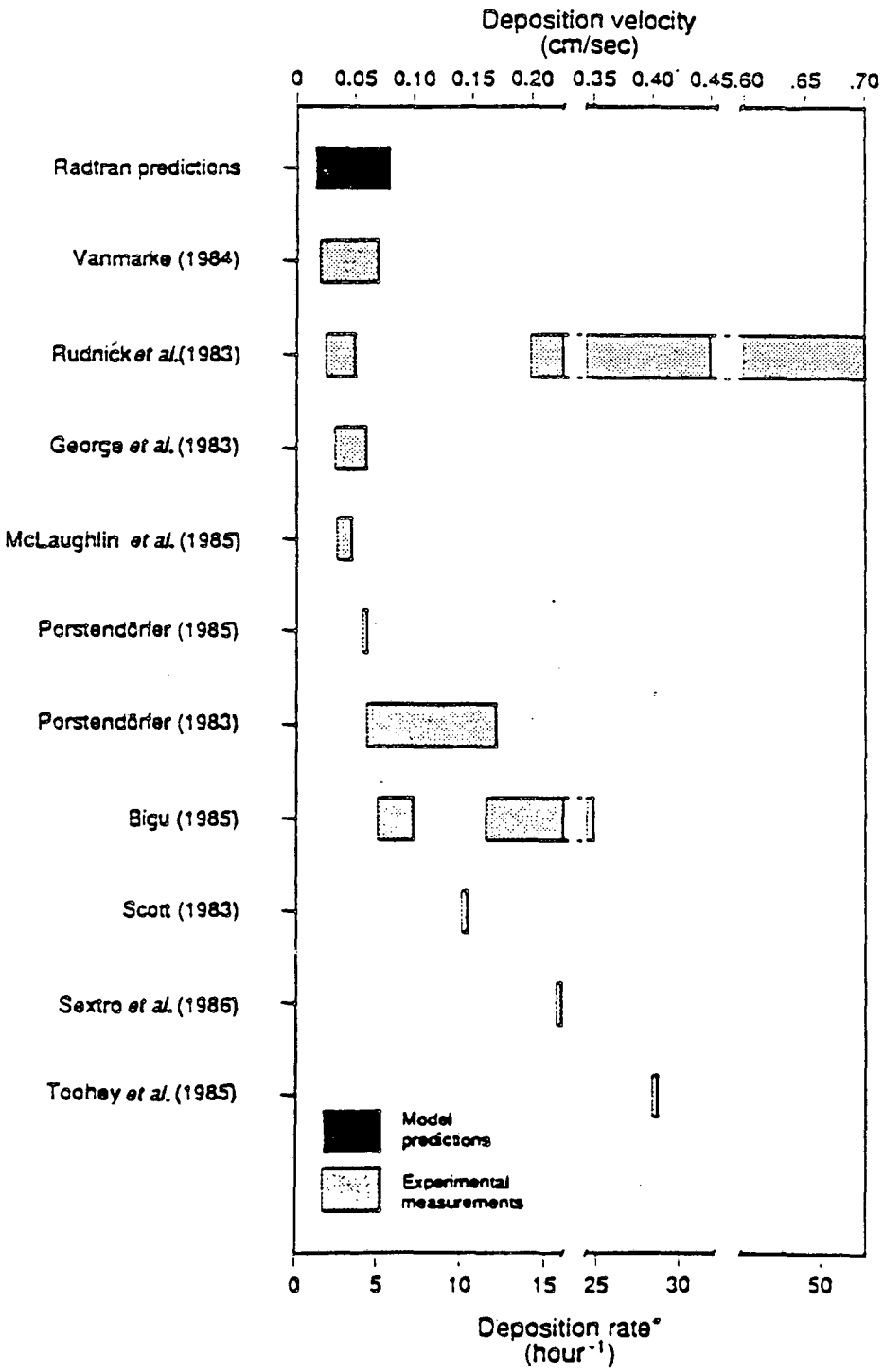


Figure 5. Free progeny deposition velocity, as predicted by RADTRAN and as measured in experiments. The range of RADTRAN predictions corresponds to the following: $D^f$ = 0.01 - 0.1 cm$^2$/sec, $X$ = 0 - 250 hr$^{-1}$, and U = 0 - 100 cm/sec

# TABLE 1

## A comparison of test conditions and experimental results

*(listed in order of increasing deposition velocity)*

| Researcher | Test Space | S/V ($m^{-1}$) | Flow Conditions | Free Deposition Velocity (cm/sec) |
|---|---|---|---|---|
| Schiller, RADTRAN | predictions | - | laminar, near-stagnant | .014-.079 |
| Vanmarke (1984) | chamber | 6.2 | minimal air flow, near-stagnant | .02 - .07 |
| Rudnick *et al.* (1983) | experimental room | 1.4 | stagnant; | .025 - .05 |
| George *et al.* (1983) | chamber | 4.7 | minimal air flow, near-stagnant | .033 - .06 |
| McLaughlin *et al.* (1985) | 50 liter cylindrical chamber | | still air | .034 - .047 |
| Porstendorfer (1985) | chamber | 5*- | closed room, turbulent U ≈ 5-17 cm/sec | .056 |
| Porstendorfer (1983) | wind tunnel | - | $U_{min}$ ≈ 10 cm/sec | .06 - .17 |
| Bigu (1985) | 26 $m^3$ chamber | - | still air | .07-.10 |
| Scott (1983) | occupied buildings | - | free convection flow U » 4-12 cm/sec | .14 |
| Bigu (1985) | 26 $m^3$ chamber | - | mixing fans, turb. | .16-.35 |
| Rudnick *et al.* (1983) | experimental room | 1.4 | mixing fans, turbulent | .20 - .70 |
| Sextro *et al.* (1986) | experimental room | 1.9 | unknown (air cleaner (fans operating) | .22 |
| Toohey (1985) | utility room of house | - | unknown | .4 |

* including furniture in the room

# APPENDIX

## One-Dimensional Diffusion Equations

*General Formulation* (for decay product i = 1, 2, 3)

Governing equations:

$$D^f \frac{d^2 A_i^f}{dy^2} = (\lambda_i + X) A_i^f - \lambda_i A_{i-1}^f - r_{i-1}\lambda_i A_{i-1}^a$$

$$D^a \frac{d^2 A_i^a}{dy^2} = \lambda_i A_i^a - X A_i^f - (1-r_{i-1})\lambda_i A_{i-1}^a$$

where:

$$A_o^f = A_o = A_{radon} \qquad A_o^a = 0$$

$$r_1 = r \qquad r_2 = r_3 = 0$$

Boundary conditions:

$$\text{at } y = 0; \qquad A_i = 0$$

$$\text{at } y \to -\infty \quad \frac{dA_i}{dy} = \frac{d^2 A_i}{dy^2} = 0 \quad A_i = A_{i_\infty}, \text{ finite}$$

Deposition velocity:

$$u_i = \frac{D}{A_{i_\infty}} \left.\frac{dA_i}{dy}\right|_{y=0}$$

Define non-dimensional concentration:

$$\theta_i = \frac{A_i}{A_o}$$

Define diffusion lengths:

$$d_i^f = \left[\frac{D^f}{\lambda_i + x}\right]^{1/2}$$

$$d_i^a = \left[\frac{D^a}{\lambda_i}\right]^{1/2}$$

*First Free Decay Product*

Non-dimensional governing equation:

$$(d\{\,)^2 \frac{d^2\theta_1^f}{dy^2} = \theta_1^f - \frac{\lambda_1}{\lambda_1+X}$$

Freestream concentration (y→∞):

$$\theta_{1_\infty}^f = \frac{\lambda_1}{\lambda_1 + X}$$

Solution:

$$\theta_1^f(y) = \theta_{1_\infty}^f [1 - \exp(-y/d\{\,)]$$

Deposition velocity:

$$u\{ = \frac{D^f}{d\{} = [D^f(\lambda_1 + X)]^{1/2}$$

*First Attached Decay Product*

Non-dimensional governing equation:

$$(d_1^a)^2 \frac{d^2\theta^a}{dy^2} = \theta_1^a - \frac{X}{\lambda_1}\theta_1^f$$

Freestream concentration (y→∞):

$$\theta_{1_\infty}^a = \frac{X}{\lambda_1}\theta_{1_\infty}^f = \frac{X}{\lambda_1 + X}$$

Solution:

$$\theta_1^a(y) = \theta_{1_\infty}^a \left[1 - \frac{(d\{\,)^2 \exp(-y/d\{\,) - (d_1^a)^2 \exp(-y/d_1^a)}{(d\{\,)^2 - (d_1^a)^2}\right]$$

Approximate solution:

(assuming $D^f >> D^a$, $d^f >> d^a$)

$$\theta_1^a(y) = \frac{\chi}{\lambda_1}\,\theta_1^f(y) = \theta_{1_\infty}^a \left[1-exp\,(-y/d_1^f)\right]$$

Deposition velocity:

$$u_1^a = \frac{D^a}{d_1^f + d_1^a} \approx \frac{D^a}{d_1^f} = \left[\frac{D^a}{D^f}\right]^{1/2} [D^a(\lambda_1 + \chi)]^{1/2}$$

*Second Free Decay Product*

Non-dimensional governing equation:

$$(d_2^f)^2\,\frac{d^2\theta_2^f}{dy^2} = \theta_2^f - \frac{\lambda_2}{\lambda_2 + \chi}\,[\theta_1^f + r\,\theta_1^a]$$

Freestream concentration ($y \to -\infty$):

$$\theta_{2_\infty}^f = \frac{\lambda_2}{\lambda_2 + \chi}\,[\theta_{1_\infty}^f + r\,\theta_{1_\infty}^a] = \frac{\lambda_2(\lambda_1 + r\chi)}{(\lambda_2 + \chi)(\lambda_1 + \chi)}$$

Solution:

$$\theta_2^f(y) = \theta_{2_\infty}^f \left[[1 - \exp(-y/d_2^f)] + \frac{(d_1^f)^2 \cdot [\exp(-y/d_1^f) - \exp(-y/d_2^f)]}{(d_2^f)^2 - (d_1^f)^2}\right]$$

Deposition velocity:

$$u_2^f = \frac{D^f}{d_2^f + d^f} = \frac{[D^f]^{1/2}}{(\lambda_2 + \chi)^{-1/2} + (\lambda_1 + \chi)^{-1/2}}$$

*Second Attached Decay Product*

Non-dimensional governing equation:

$$(d_2^a)^2\,\frac{d^2\theta_2^a}{dy^2} = \theta_2^a - \frac{\chi}{\lambda_2}\theta_2^f - (1 - r)\theta_1^a$$

Freestream concentration ($y \rightarrow -\infty$):

$$\theta_{2_{-\infty}}^{a} = \frac{X}{\lambda_2}\,\theta_{2_{-\infty}}^{f} + (1-r)\theta_{1_{-\infty}}^{a} = \frac{X(\lambda_1 + rX)}{(\lambda_2 + X)(\lambda_1 + X)} + \frac{X(1-r)}{(\lambda_1 + X)}$$

Approximate solution:

(assuming $D^f >> D^a$, $d^f >> d^a$)

$$\theta_2^a(y) = \frac{X}{\lambda_2}\theta_2^f(y) + (1-r)\theta_1^a(y)$$

(see previous expressions for $\theta_2^f(y)$ and $\theta_1^a(y)$)

Deposition velocity:

$$u_2^a = \frac{D^a}{\theta_{2_{-\infty}}^{a}}\left[\frac{X}{\lambda_2}\,\theta_{2_{-\infty}}^{f} u_2^f + (1-r)\theta_{1_{-\infty}}^{a} u_1^a\right]$$

(see previous expressions)

*Third Free Decay Product*

Non-dimensional governing equation:

$$(d_3^f)^2 \frac{d^2\theta_3^f}{dy^2} = \theta_3^f - \frac{\lambda_3}{\lambda_3 + X}\theta_2^f$$

Freestream concentration ($y \rightarrow -\infty$):

$$\theta_{3_{-\infty}}^{f} = \frac{\lambda_3}{\lambda_3 + X}\theta_{2_{-\infty}}^{f} = \frac{\lambda_3\lambda_2(\lambda_1 + rX)}{(\lambda_3 + X)(\lambda_2 + X)(\lambda_1 + X)}$$

Solution:

$$\theta_3^f(y) = \theta_{3_{-\infty}}^{f}\left[\left[1 - \exp(-y/d_3^f)\right] + \frac{(d_2^f)^4\left[\exp(-y/d_3^f) - \exp(-y/d_2^f)\right]}{\left[(d_2^f)^2 - (d_1^f)^2\right]\cdot\left[(d_2^f)^2 - (d_3^f)^2\right]}\right.$$

$$\left. + \frac{(d_1^f)^4\left[\exp(-y/d_3^f) - \exp(-y/d_1^f)\right]}{\left[(d_1^f)^2 - (d_2^f)^2\right]\cdot\left[(d_1^f)^2 - (d_3^f)^2\right]}\right]$$

Deposition velocity:

$$u_3^f = D^f \left\{ \frac{1}{d_3^f} + \frac{(d_2^f)^4}{[(d_2^f)^2 - (d_1^f)^2] \cdot [(d_2^f)^2 - (d_3^f)^2]} \left[ \frac{1}{d_2^f} - \frac{1}{d_3^f} \right] \right.$$

$$\left. + \frac{(d_1^f)^4}{[(d_1^f)^2 - (d_2^f)^2] \cdot [(d_1^f)^2 - (d_3^f)^2]} \left[ \frac{1}{d_1^f} - \frac{1}{d_3^f} \right] \right\}$$

*Third Attached Decay Product*

Non-dimensional governing equation:

$$(d_3^a)^2 \frac{d^2\theta_3^a}{dy^2} = \theta_3^a - \frac{X\theta_3^f}{\lambda_3} - \theta_2^a$$

Freestream concentration ( $y \to \infty$):

$$\theta_{3_\infty}^a = \frac{X}{\lambda_3} \theta_{3_\infty}^f + \theta_{2_\infty}^a$$

$$= \frac{X\lambda_2(\lambda_1 + rX)}{(\lambda_3 + X)(\lambda_2 + X)(\lambda_1 + X)} + \frac{X(\lambda_1 + rX)}{(\lambda_2 + X)(\lambda_1 + X)} + \frac{X(1-r)}{(\lambda_1 + X)}$$

Approximate solution:

(assuming $D^f >> D^a$, $d^f >> d^a$)

$$\theta_3^a(y) = \frac{X}{\lambda_3}\theta_3^f(y) + \theta_2^a(y)$$

(see previous expressions for $\theta_3^f(y)$ and $\theta_2^a(y)$)

Deposition velocity:

$$u_3^a = \frac{D^a}{\theta_{3_\infty}^a} \left[ \frac{X}{\lambda_3} \theta_{3_\infty}^f u_3^f + \theta_{2_\infty}^a u_2^a \right]$$

LAWRENCE BERKELEY LABORATORY
TECHNICAL INFORMATION DEPARTMENT
1 CYCLOTRON ROAD
BERKELEY, CALIFORNIA 94720